Journal of the Egyptian Mathematical Society (2012) **20**, 235–241

Egyptian Mathematical Society

Journal of the Egyptian Mathematical Society

www.etms-eg.org
www.elsevier.com/locate/joems

ORIGINAL ARTICLE

Optical bistability outside the rotating wave approximation in mixed species

M.F.M. Ali

Ain Shams University, Faculty of Science, Department of Mathematics, Cairo, Egypt

Received 14 January 2012; accepted 21 May 2012
Available online 2 September 2012

KEYWORDS

Optical bistability;
Rotating wave approximation

Abstract Optical bistable behavior for a system of inhomogeneously broadened two sorts of two-level atoms in a ring cavity is investigated outside the rotating wave approximation (RWA). The model Maxwell–Bloch equations are treated with Fourier decomposition up to first harmonic. The first harmonic output field component exhibits reversed or mushroom bistability simultaneously with bi- and double-bistability in the fundamental field component. Inhomogeneous broadening and transverse field effects are also considered.

1. Introduction

Optical bistability (OB) phenomenon has potential applications in optical communication and quantum processing of information. This phenomenon has been investigated for a homogeneously broadened two-level atomic medium placed inside an optical cavity in the plane wave approximation [1–16]. Investigation of OB systems within the plane wave approximation, where the homogeneously broadened atomic system is in interaction with a squeezed vacuum input field has been studied in [17–27]. Further, transverse effect of the radiation field in OB systems with homogeneously and inhomogeneously broadened two-level atoms has been examined [28–34].

On the other hand, optical tristability arise when the ring cavity contains a homogeneously mixed atomic species in the plane wave approximation [35,36]. Also, the steady state behavior of a bistable system of a homogeneously or inhomogeneously broadened mixed atomic species has been analyzed, where the transverse effect of radiation field is taken into account [37].

In all previous works [1–37], rotating wave approximation (RWA) has been used, where rapidly oscillating terms (terms which oscillate at twice the driving field frequency) are neglected. Optical bistability for a homogeneously two-level atomic system in a ring cavity in the plane wave approximation has been investigated recently outside the RWA [38] where the non-autonomous model Maxwell–Bloch equations are treated with Fourier decomposition up to first harmonic (cf. [39]).

In the present work, we investigate the OB outside the RWA for a system of inhomogeneously broadened two sorts of two-level atoms placed in a ring cavity (Fig. 1), where the transverse profile of the incident coherent field is considered. A realistic model can be a mixture of two metal vapors like

E-mail address: dr.mona.fathy@hotmail.com

Peer review under responsibility of Egyptian Mathematical Society.

ELSEVIER Production and hosting by Elsevier

1110-256X © 2012 Egyptian Mathematical Society. Production and hosting by Elsevier B.V. Open access under CC BY-NC-ND license.
http://dx.doi.org/10.1016/j.joems.2012.05.002

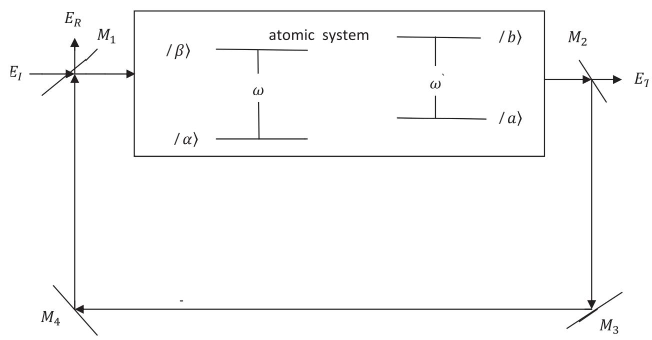

Fig. 1 The ring cavity configuration.

Potassium has an 8d level lying 1.67 cm^{-1} below the 16d level of rubidium at around 33,180 cm^{-1} (cf. [35]).

The paper is presented as follows: The non autonomous model of Maxwell–Bloch equations outside the RWA are given in Section 2. The Fourier decomposition series to solve the non-autonomous model equations for the output field up to first harmonic and to $O(\lambda)$(λ is the ratio of the Einstein A-coefficient to the input field circular frequency) is presented in Section 3. Computational results are discussed in Section 4 followed by a summary in Section 5.

2. Model equations

Consider a coherent beam E_I of frequency ω_L that is injected into a ring cavity of length L_t (Fig. 1) with E_T is the transmitted field. A large number N of two sorts of two level atoms with central transitional frequencies ω_a, ω'_a, dipole moments μ, μ', weights w_1, w_2 and longitudinal and transverse decay ratios γ_{11}, γ'_{11} and $\gamma_\perp$, $\gamma'_\perp$ is contained in a cylindrical sample of length L and radius r_0 (Fig. 1). The reduced Maxwell–Bloch equations with the one-transverse mode and mean field approximations [8,9] within the RWA [37] now takes the following form outside RWA,

$$\frac{dx}{dt} = k\left\{y-(1+i\theta)x+2C\sqrt{\frac{\gamma_\perp}{\gamma_{11}}}\frac{w_1}{w_1+w_2} \times \int_h^1 a^{-\frac{1}{2}}da\int_{-\infty}^{\infty}\left[r_-G_1(\omega)d\omega+\frac{w_2}{w_1}\frac{\mu'}{\mu}s_-G_2(\omega')d\omega'\right]\right\} \quad (1a)$$

$$\frac{\partial r_-}{\partial t} = -\gamma_\perp(1+i\Delta(\omega))r_- + \sqrt{\gamma_{11}\gamma_\perp}a^{\frac{1}{2}}r_3(x+x^*e^{i\eta t}) \quad (1b)$$

$$\frac{\partial r_3}{\partial t} = -\frac{\sqrt{\gamma_{11}\gamma_\perp}}{2}a^{\frac{1}{2}}\left[r_+(x+x^*e^{i\eta t})+r_-(x^*+xe^{-i\eta t})\right]-\gamma_{11}(r_3+1) \quad (1c)$$

$$\frac{\partial s_-}{\partial t} = -\gamma'_\perp(1+i\Delta'(\omega'))s_- + \frac{\mu'}{\mu}\sqrt{\gamma_{11}\gamma_\perp}a^{\frac{1}{2}}s_3(x+x^*e^{i\eta t}) \quad (1d)$$

$$\frac{\partial s_3}{\partial t} = -\frac{\mu'\sqrt{\gamma_{11}\gamma_\perp}}{2\mu}a^{\frac{1}{2}}\left[s_+(x+x^*e^{i\eta t})+s_-(x^*+xe^{-i\eta t})\right]-\gamma'_{11}(s_3+1) \quad (1e)$$

The notations are: $r_-\equiv r_-(\omega,r,z,t)$, $s_-\equiv s_-(\omega',r,z,t)$ and $r_3\equiv r_3(\omega,r,z,t), s_3\equiv s_3(\omega',r,z,t)$ are the mean atomic polarization components and the mean atomic population for the two types of atoms. The quantities x and y are the normalized output and input field amplitudes respectively, $C=\frac{\alpha L}{2T}$ is the cooperative parameter, $\Delta(\omega)=\frac{\omega-\omega_L}{\gamma'_\perp}$, $\Delta'(\omega')=\frac{\omega'-\omega_L}{\gamma'_\perp}$, $\eta=2\omega_L$, $\theta=\frac{\omega_c-\omega_0}{k}$ is the normalized cavity detuning, ω_c is the frequency of the cavity mode, and $k=\frac{c}{L_t}$ is the cavity decay rate.The Gaussian function $a(r)=e^{-2r^2/w_0^2}$ measures the transverse effect, $h=a(r_0)$ and $G_1(\omega)$, $G_2(\omega')$ are the distribution functions of the atomic frequencies for both types of atoms.The terms containing $e^{\pm i\eta t}$ in Eqs. (1b)–(1e) represent the effect of interaction of the cavity field with the atoms outside the RWA.Within the RWA these terms are discarded and Eq. (1) give the input-output field steady state equation [37],

$$Y = X\left|(1+i\theta)+\frac{2C}{X}\frac{w_1}{w_1+w_2}A\right|^2$$

$$A=(1-i\Delta_a)\ln g_1(X)+\sigma'_1 ln\frac{g_2(X)}{g_2^*(X)} + \frac{w_2}{w_1}\frac{\gamma'_{11}}{\gamma_{11}}\left[(1-i\Delta'_a)lng'_1(X)+\sigma'_2 ln\frac{g'_2(X)}{g'^*_2(X)}\right] \quad (2)$$

where $X=|x_0|^2$ and $Y=|y|^2$ are the fundamental output and input field intensities and the distribution functions of the atomic frequencies are taken Lorentzian of peak frequencies ω_a, ω'_a, i.e.,

$$G_1(\omega)=\frac{\sigma_1/\pi}{(\omega-\omega_a)^2+\sigma_1^2},\quad G_2(\omega')=\frac{\sigma_2/\pi}{(\omega'-\omega'_a)^2+\sigma_2^2}.$$

$$g_1(X)=\frac{\Delta_a^2+(\sigma'_1+B_1)^2}{\Delta_a^2+(\sigma'_1+B_2)^2},\quad g'_1(X)=\frac{\Delta'^2_a+(\sigma'_2+B'_1)^2}{\Delta'^2_a+(\sigma'_2+B'_2)^2},$$

$$g_2(X)=\Delta_a^2+i\Delta_a(B_1-B_2)+(\sigma'_1+B_1)(\sigma'_1+B_2),$$

$$g'_2(X)=\Delta'^2_a+i\Delta'_a(B'_1-B'_2)+(\sigma'_2+B'_1)(\sigma'_2+B'_2),$$

$$B_1=\sqrt{1+X},\quad B_2=\sqrt{1+hX},$$

$$B'_1=\sqrt{1+\frac{(1+\Delta'^2_a)}{b'(1+\Delta_a^2)}X},\quad B'_2=\sqrt{1+\frac{h(1+\Delta'^2_a)}{b'(1+\Delta_a^2)}X},$$

$$b(\omega,\omega')=\frac{\mu^2\gamma'_{11}\gamma'_\perp}{\mu'^2\gamma_{11}\gamma_\perp}\frac{(1+\Delta'^2(\omega'))}{(1+\Delta^2(\omega))},\quad b'\equiv b(\Delta=\Delta_a,\Delta'=\Delta'_a),$$

$\Delta_a\equiv\Delta(\omega=\omega_a)$, $\Delta'_a\equiv\Delta'(\omega'=\omega'_a)$ and the normalized widths

$$\sigma'_1=\frac{\sigma_1}{\gamma_\perp},$$

$$\sigma'_2=\frac{\sigma_2}{\gamma'_\perp}.$$

Next, we analyze the non-autonomous system (1) to reach a formula for the additional first harmonic component of the output field outside the RWA.

3. Analytical solution outside the RWA

The solution of Eq. (1) for the atomic Bloch components and the cavity field x contains all harmonics of frequency $2\omega_L n$, where n is an integer, due to the presence of the time dependent coefficients $e^{\pm i\eta t}$. We assume, up to first harmonic ($n=\pm1$), the following Fourier decomposition formula [38–40],

$$r_{\mp,3}=r^0_{\mp,3}+r^+_{\mp,3}e^{i\eta t}+r^-_{\mp,3}e^{-i\eta t}, \quad (3a)$$

$$s_{\mp,3}=s^0_{\mp,3}+s^+_{\mp,3}e^{i\eta t}+s^-_{\mp,3}e^{-i\eta t}, \quad (3b)$$

$$x(t)=x_0(t)+x_+(t)e^{i\eta t}+x_-(t)e^{-i\eta t}, \quad (3c)$$

where $r^0_\mp(\omega,r,z,t)$, $s^0_\mp(\omega',r,z,t)$, $x_0(t)$ are the fundamental atomic and field components respectively within the RWA,

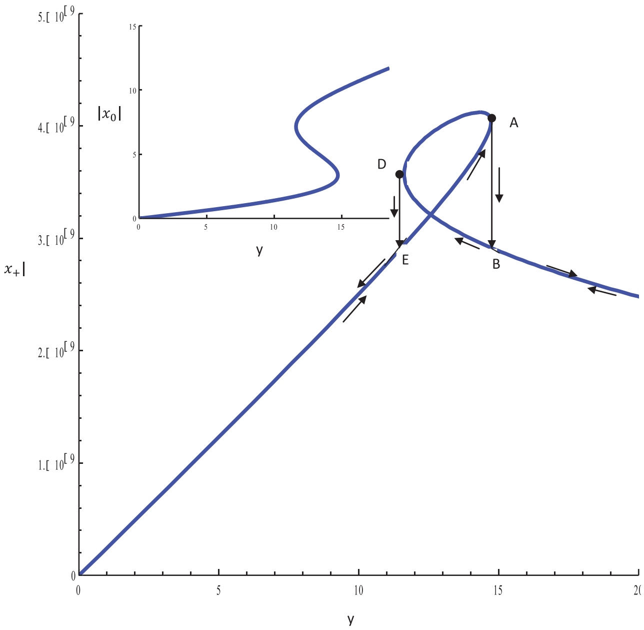

Fig. 2 The first harmonic component $|x_+|$ of the output field against the input field y for one sort of atom: $C = 20,\ \varDelta_a = 4,\ \varDelta'_a = 4,\ \theta = 2,\ \lambda_1 = \lambda_2 = 0.5 \times 10^{-6},\ k = 100\gamma_\perp$.

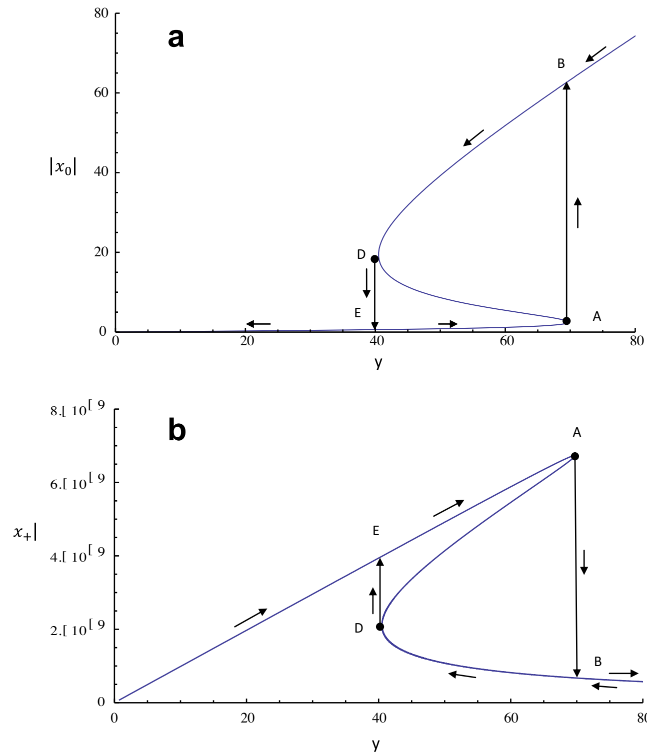

Fig. 3 (a) The fundamental field component $|x_0|$ against y for $C = 100,\ \varDelta_a = \varDelta'_a = \theta = \sigma'_1 = \sigma'_2 = 0,\ \lambda_1 = \lambda_2 = 10^{-6},\ \ k = 100\gamma_\perp,\ \frac{r_0}{w_0} = 1,\ b' = 7,\ \frac{\gamma'_{11}}{\gamma_{11}} = 1.1,\ \frac{w_2}{w_1} = 2$. (b) The first harmonic component $|x_+|$ against y for the same data as (a).

$r^+_\mp(\omega, r, z, t), r^-_\mp(\omega, r, z, t),\ s^+_\mp(\omega', r, z, t) s^-_\mp(\omega', r, z, t)$ and $x_\mp(t)$ are the additional first harmonic components outside the RWA.

Substituting Eq. (3) into (1) and comparing the different coefficients of $e^{\pm in\eta t}$ $(n = 0, 1)$, we get in the steady state the following system of equations for the fundamental and first harmonic components,

$$r^0_- = \sqrt{\frac{\gamma_{11}}{\gamma_\perp}} \frac{1}{(1 + i\varDelta(\omega))} \left[r^0_3 (x_0 + x^*_+) + r^-_3 (x^*_0 + x_+) + r^+_3 x_- \right] = (r^0_+)^* \tag{4a}$$

$$r^+_- = \sqrt{\frac{\gamma_{11}}{\gamma_\perp}} \frac{1}{\left(1 + i\varDelta(\omega) + \frac{i}{\lambda_1}\right)} \left[r^0_3 (x^*_0 + x_+) + r^+_3 (x_0 + x^*_+) + r^-_3 x^*_- \right] = (r^-_+)^* \tag{4b}$$

$$r^-_- = \sqrt{\frac{\gamma_{11}}{\gamma_\perp}} \frac{1}{\left(1 + i\varDelta(\omega) - \frac{i}{\lambda_1}\right)} \left[r^0_3 x_- + r^-_3 (x_0 + x^*_+) \right] = (r^+_+)^* \tag{4c}$$

$$r^0_3 = -1 - \frac{1}{2} \sqrt{\frac{\gamma_\perp}{\gamma_{11}}} \left[(r^0_+ + r^+_-)(x_0 + x^*_+) + (r^0_- + r^-_+)(x^*_0 + x_+) + r^+_+ x_- + r^-_- x^*_- \right] \tag{4d}$$

$$r^+_3 = -\frac{1}{2} \sqrt{\frac{\gamma_\perp}{\gamma_{11}}} \frac{1}{\left(1 + i\frac{\gamma_\perp}{\gamma_{11}\lambda_1}\right)} \left[(r^0_+ + r^+_-)(x^*_0 + x_+) + r^+_+ (x_0 + x^*_+) + r^-_+ x^*_- + r^0_- x^*_- \right] = (r^-_3)^* \tag{4e}$$

$$s^0_- = \frac{\sqrt{\gamma_{11}\gamma_\perp}}{\gamma'_\perp} \frac{\mu'}{\mu} \frac{1}{(1 + i\varDelta'(\omega'))} \times \left[s^0_3 (x_0 + x^*_+) + s^-_3 (x^*_0 + x_+) + s^+_3 x_- \right] = (s^0_+)^* \tag{5a}$$

$$s^+_- = \frac{\sqrt{\gamma_{11}\gamma_\perp}}{\gamma'_\perp} \frac{\mu'}{\mu} \frac{1}{(1 + i\varDelta'(\omega') + i/\lambda_2)} \times \left[s^0_3 (x^*_0 + x_+) + s^+_3 (x_0 + x^*_+) + s^-_3 x^*_- \right] = (s^-_+)^* \tag{5b}$$

$$s^-_- = \frac{\sqrt{\gamma_{11}\gamma_\perp}}{\gamma'_\perp} \frac{\mu'}{\mu} \frac{1}{(1 + i\varDelta'(\omega') - i/\lambda_2)} \left[s^0_3 x_- + s^-_3 (x_0 + x^*_+) \right] = (s^+_+)^* \tag{5c}$$

$$s^0_3 = -1 - \frac{1}{2} \frac{\sqrt{\gamma_{11}\gamma_\perp}}{\gamma'_{11}} \frac{\mu'}{\mu} \left[(s^0_+ + s^+_-)(x_0 + x^*_+) + (s^0_- + s^-_+)(x^*_0 + x_+) + s^+_+ x_- + s^-_- x^*_- \right] \tag{5d}$$

$$s^+_3 = -\frac{1}{2} \frac{\mu'}{\mu} \frac{\sqrt{\gamma_{11}\gamma_\perp}}{\gamma'_{11}} \frac{1}{\left(1 + i\frac{\gamma'_\perp}{\gamma'_{11}\lambda_2}\right)} \times \left[(s^0_+ + s^+_-)(x^*_0 + x_+) + s^+_+ (x_0 + x^*_+) + s^-_+ x^*_- + s^0_- x^*_- \right] = (s^-_3)^* \tag{5e}$$

$$y = (1 + i\theta) x_0 - 2C \sqrt{\frac{\gamma_\perp}{\gamma_{11}}} \frac{w_1}{w_1 + w_2} \int_h^1 a^{-\frac{1}{2}} da \times \int_{-\infty}^{\infty} \left[r^0_- G_1(\omega) d\omega + \frac{w_2}{w_1} \frac{\mu'}{\mu} s^0_- G_2(\omega') d\omega' \right] \tag{6a}$$

$$x_\pm = \frac{2C}{\varDelta_\pm} \sqrt{\frac{\gamma_\perp}{\gamma_{11}}} \frac{w_1}{w_1 + w_2} \int_h^1 a^{-\frac{1}{2}} da \times \int_{-\infty}^{\infty} \left[r^\pm_- G_1(\omega) d\omega + \frac{w_2}{w_1} \frac{\mu'}{\mu} s^\pm_- G_2(\omega') d\omega' \right] \tag{6b}$$

where $\Lambda_{\pm} = 1 + i\left(\theta \pm \frac{1}{v}\right),\ \lambda_1 = \frac{\gamma_\perp}{\eta},\ \lambda_2 = \frac{\gamma'_\perp}{\eta},\ v = \frac{k}{\eta}$.

Eq. (6a) with Lorentzian frequency distributions reduce to the input-output field state equation (within RWA), Eq. (2). Substituting Eq. (6b) for $x_\pm$ into Eqs. (4b) and (5b) and solving the resulting equation with Eqs. (4e) and (5e) up to $O(\lambda_i)$; $i = 1,2$ [40], the steady state values of r_-^+ and s_-^+ are,

$$r_-^+ = \sqrt{\frac{\gamma_{11}}{\gamma_\perp}}\frac{r_3^0 x_0^*}{[1 + i(\Delta(\omega) + 1/\lambda_1)]} = \frac{(1 - i\Delta(\omega))r_+^0}{[1 + i(\Delta(\omega) + 1/\lambda_1)]} = \left(r_+^-\right)^* \tag{7a}$$

$$\begin{aligned} s_-^+ &= \frac{\sqrt{\gamma_{11}\gamma_\perp}}{\gamma'_\perp}\frac{\mu'}{\mu}\frac{s_3^0 x_0^*}{[1 + i(\Delta'(\omega') + 1/\lambda_2)]} \\ &= \frac{(1 - i\Delta'(\omega'))s_+^0}{[1 + i(\Delta'(\omega') + 1/\lambda_2)]} = \left(s_+^-\right)^* \end{aligned} \tag{7b}$$

The components $r_+^0,\ s_+^0$ as solved by the system of Eqs. (4,5,6) up to $O(\lambda_i)$; $i = 1,2$ are actually the quadrature polarization components within the RWA [37], i.e.,

$$r_+^0 = -\sqrt{\frac{\gamma_{11}}{\gamma_\perp}}\frac{(1 + i\Delta(\omega))a^{\frac{1}{2}}x_0^*}{\left[1 + \Delta^2(\omega) + a|x_0|^2\right]} = (r_-^0)^* \tag{8a}$$

$$s_+^0 = -\frac{\gamma'_{11}}{\sqrt{\gamma_{11}\gamma_\perp}}\frac{\mu}{\mu'}\frac{(1 + i\Delta'(\omega'))a^{\frac{1}{2}}x_0^*}{\left[b(\omega,\omega')(1 + \Delta^2(\omega)) + a|x_0|^2\right]} = \left(s_-^0\right)^* \tag{8b}$$

From Eqs. (6b), (7), and (8), we get the expression for the field component x_+,

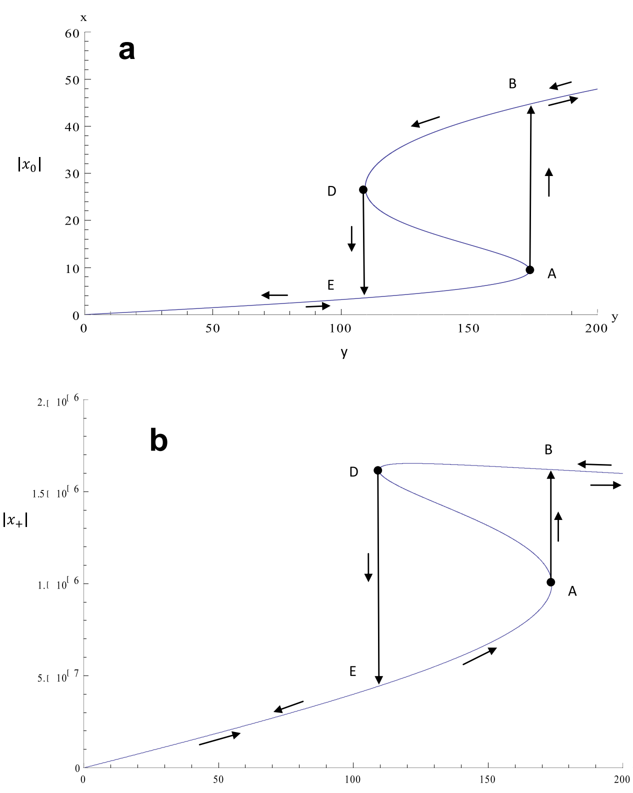

Fig. 4 (a) The fundamental field component $|x_0|$ against y for $C = 1000,\ \Delta_a{=}10,\ \Delta'_a{=}-20,\ \theta{=}-12,\ \lambda_1{=}\lambda_2{=}10^{-6},\ k = 100\gamma_\perp,\ \sigma'_1 = 0.2,\ \sigma'_2 = 0.5,\ \frac{r_0}{w_0} = 1,\ b' = 7,\ \frac{\gamma'_{11}}{\gamma_{11}} = 1.1,\ \frac{w_2}{w_1} = 2$. (b) The first harmonic component $|x_+|$ against y for the same data as (a).

$$x_+ = -\frac{2C}{\Lambda_+}\frac{w_1}{w_1 + w_2}x_0^*\int_h^1 da\int_{-\infty}^{\infty}\left[A_1(\omega)d\omega + \frac{w_2}{w_1}\frac{\gamma'_{11}}{\gamma_{11}}A_2(\omega')d\omega'\right] \tag{9}$$

where $\mathrm{A}_1(\omega) = \frac{(1+\Delta^2(\omega))\mathrm{G}_1(\omega)}{\left[1+\mathrm{i}(\Delta(\omega)+\frac{1}{\lambda_1})\right]\left[1+\Delta^2(\omega)+\mathrm{a}|\mathrm{x}_0|^2\right]}$,

$$\mathrm{A}_2(\omega') = \frac{(1 + \Delta'^2(\omega'))\mathrm{G}_2(\omega')}{[1 + \mathrm{i}(\Delta'(\omega') + 1/\lambda_2)]\left[\mathrm{m}(1 + \Delta'^2(\omega') + \mathrm{a}|\mathrm{x}_0|^2)\right]},$$

$$m = \frac{1 + \Delta_a^2}{1 + \Delta_a'^2}b'.$$

Up to (λ_i); $i = 1,2$, we have $x_- = 0$.

In the case where the distribution functions of the atomic frequencies $G_1(\omega)$, $G_2(\omega')$ are Lorentzians, Eq. (9) takes the form,

$$\begin{aligned} x_+ = &-\frac{2Cx_0^*}{\Lambda_+|x_0|^2}\frac{w_1}{w_1 + w_2}\left\{\frac{2\sigma'_1(1 + a_1^2)}{|V_2|^2}ln\frac{B_1 + a_1 i}{B_2 + a_1 i}\right. \\ &+\left(\frac{V_1}{V_2}\right)^* ln\frac{K_2}{K_1} + \frac{V_1}{V_2}ln\left(\frac{K_1}{K_2}\right)^* + \frac{w_2}{w_1}\frac{\gamma'_{11}}{\gamma_{11}} \\ &\left.\left[\frac{2\sigma'_2(1 + a_2^2)}{|V'_2|^2}ln\frac{B'_1 + a_2 i}{B'_2 + a_2 i} + \left(\frac{V'_1}{V'_2}\right)^* ln\frac{K'_2}{K'_1} + \frac{V'_1}{V'_2}ln\left(\frac{K'_1}{K'_2}\right)^*\right]\right\} \end{aligned} \tag{10}$$

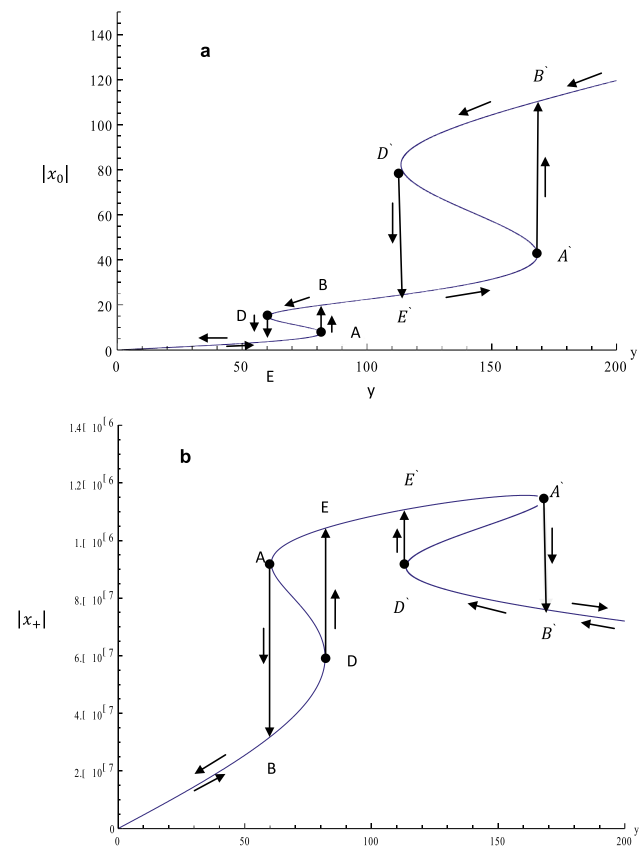

Fig. 5 (a) The fundamental field component $|x_0|$ against y for $C = 700,\ \Delta_a{=}10,\ \Delta'_a{=}-20,\ \theta{=}-3,\ \lambda_1{=}\lambda_2 = 10^{-6},\ k = 100\gamma_\perp,\ \sigma'_1 = 0.2,\ \sigma'_2 = 0.5,\ \frac{r_0}{w_0} = 1,\ b' = 7,\ \frac{\gamma'_{11}}{\gamma_{11}} = 1.1,\ \frac{w_2}{w_1} = 2$. (b) The first harmonic component $|x_+|$ against y for the same data as (a).

where

$$a_1 = \frac{1}{\lambda_1} - \mathrm{i}, \quad a_2 = \frac{1}{\lambda_2} - \mathrm{i}, \quad K_1 = B_1^+\sigma_1' - i\Delta_a, K_2 = B_2^+\sigma_1' - i\Delta_a,$$
$$K_1' = B_1' + \sigma_2' - i\Delta_a', \quad K_2' = B_2' + \sigma_2' - i\Delta_a',$$
$$V_1 = 1 - \left(\sigma_1' + i\Delta_a\right)^2,$$
$$V_1' = 1 - \left(\sigma_2' + i\Delta_a'\right)^2, \quad V_2 = \sigma_1' + i(\Delta_a + a_1),$$
$$V_2' = \sigma_2' + i\left(\Delta_a' + a_2\right).$$

In the case of homogeneous broadening $\left(\sigma_1' = \sigma_2' = 0\right)$ and in the plane wave approximation limit, where $\frac{r_0}{w_0} \to 0$, $C \to \infty$ with $C' = 2C\left(\frac{r_0}{w_0}\right)^2$ fixed, Eq. (10) reduces to,

$$x_+ = -\frac{2Cx_0^*}{\Delta_+}\frac{w_1}{w_1 + w_2}\left\{\frac{1 + \Delta_a^2}{\left[1 + i\left(\Delta_a^+ 1/\lambda_1\right)\right]\left[1 + \Delta_a^2 + |x_0|^2\right]} + \frac{w_2}{w_1}\frac{\gamma_{11}'}{\gamma_{11}}\frac{1 + \Delta_a'^2}{\left[1 + i\left(\Delta_a' + 1/\lambda_2\right)\right]\left[b'\left(1 + \Delta_a^2\right) + |x_0|^2\right]}\right\} \quad (11)$$

The comparison between the behavior of the first harmonic field component x_+ arise outside the RWA, Eq. (10), and the fundamental field component x_0 (within the RWA, Eq. (2)) against the input field y is presented next.

4. Results and discussion

First, for the case of one sort of atom, $b = \frac{w_2}{w_1} = \frac{\gamma_{11}'}{\gamma_{11}} = 1$, and homogeneous broadening in the plane wave approximation with $C = 20$, $\Delta_a = \Delta_a' = 4$, $\theta = 2, \lambda = \lambda' = 0.5 \times 10^{-6}$, $k = 100\gamma_\perp$ (Fig. 2), the first harmonic field component $|x_+|$ shows butterfly (knotted) OB shape which *confirms* the results obtained in [38] for two-level atomic system.

At exact resonance ($\Delta_a = \Delta_a' = \theta = 0$) and for $C = 100$ with inhomogeneous broadening and transverse field effects, the field component $|x_+|$ exhibits reversed (clockwise) bistable behavior compared with the usual (anti-clockwise) bistable behavior for $|x_0|$ (Fig. 3). In Fig. 3a points A, D represent switch on and off for $|x_0|$ while in Fig. 3b points A, D represent the reverse order of switching for $|x_+|$.

In the dispersive case, where the atomic and cavity detuning have opposite signs and for higher value of $C = 1000$, both field components $|x_+|$ and $|x_0|$ exhibit the usual (anti-clockwise) bistable behavior (Fig. 4) with $|x_+|$ shows slow decrease after the switch-up process (to the right of point D). For lesser $C = 700$, the field component $|x_0|$ shows double bistable (multi-stable) behavior (Fig. 5a) while the field component $|x_+|$ shows asymmetric mushroom structure (Fig. 5b), with two-way switching-up and -down processes.

Now, for other values of the damping constants $k = \gamma_\perp$ and $k = 10^{-2}\gamma_\perp$, the field component $|x_0|$ is independent of this ratio, but the field component $|x_+|$, Fig. 6, is smaller in the case $k = 10^{-2}\gamma_\perp$.

Finally, the dependence of the field component $|x_+|$ on the parameter $\lambda(=\lambda_{1,2})$ shows a rapid increase in the dispersive and inhomogeneous broadening case, Fig. 7a, compared with slower increase in the absorptive homogeneous case, Fig. 7b.

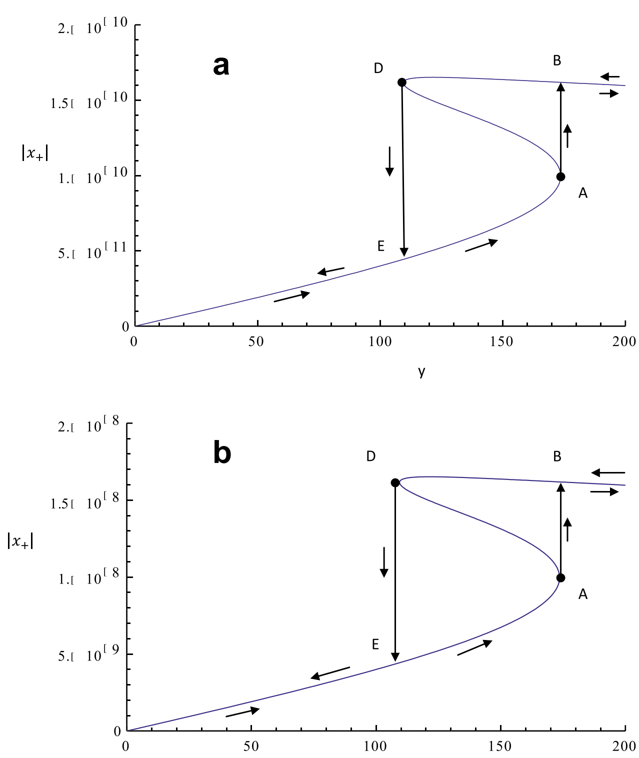

Fig. 6 Same as Fig. 4b but for (a) $k = 10^{-2}\gamma_\perp$, (b) $k = \gamma_\perp$.

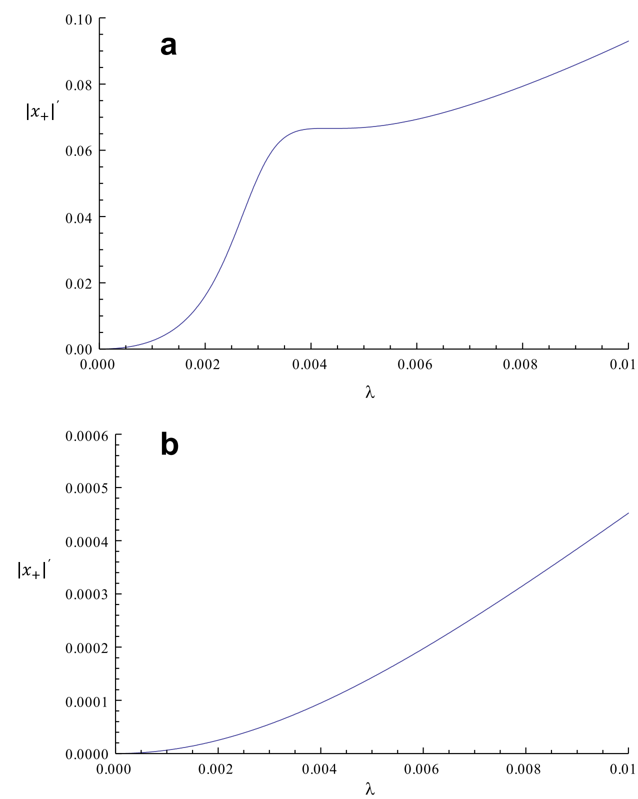

Fig. 7 The scaled first harmonic field component $|x_+|'\left(|x_+|' = \frac{|x_+|}{2C}\frac{w_1+w_2}{w_1}\right)$ against the parameter $\lambda(=\lambda_{1,2})$ for fixed value of $|x_0| = 100$ and for $C = 700$, $k = 100\gamma_\perp$, $\frac{r_0}{w_0} = 1$, $b' = 7$, $\frac{\gamma_{11}'}{\gamma_{11}} = 1.1$, $\frac{w_2}{w_1} = 2$. (a)$\Delta_a = 10$, $\Delta_a' = -20$, $\theta = -3$, $\sigma_1' = 0.2$, $\sigma_2' = 0.5$. (b) $\Delta_a = \Delta_a' = \theta = \sigma_1' = \sigma_2' = 0$.

5. Summary

Optical bistable behavior for a system of inhomogeneously broadened two sorts of two level atoms placed in a ring cavity with the transverse effect of the radiation field is investigated outside the RWA using Maxwell–Bloch equations with Fourier decomposition up to first harmonic. The first harmonic output field component exhibits reversed or mushroom bistability simultaneously with bistability or double bistability in the fundamental field component depending on the control of the system parameters. In all cases, the additional first harmonic field is small $O(\lambda_i)$; $i = 1, 2$, compared with the fundamental component. As stated in [39], the detection of this weak first harmonic field can be achieved, for example, with phase sensitive detection technique similar to that used in detecting squeezed light [41].

Acknowledgment

I would like to thank Professor S.S. Hassan and Dr. Y.A. Sharaby for their interest in the work.

References

[1] R. Bonifacio, L.A. Lugiato, Cooperative effects and bistability for resonance fluorescence, Opt. Commun. 19 (1976) 172–176.
[2] R. Bonifacio, L.A. Lugiato, Optical bistability and cooperative effects in resonance fluorescence, Phys. Rev. A 18 (1978) 1129–1144.
[3] R. Bonifacio, L.A. Lugiato, Bistable absorption in a ring cavity, Lett. Nuovo Cimento 21 (1978) 505–509.
[4] S.L. McCall, Instabilities in continuous-wave light propagation in absorbing media, Phys. Rev. A 9 (1974) 1515–1523.
[5] S.L. McCall, H.M. Gibbs, Standing wave effects in optical bistability, Opt. Commun. 33 (1980) 335–339.
[6] R. Bonifacio, L.A. Lugiato, Instabilities for a coherently driven absorber in a ring cavity, Lett. Nuovo Cimento 21 (1978) 510–516.
[7] R. Bonifacio, M. Gronchi, L.A. Lugiato, Dispersive bistability in homogeneously broadened systems, Lett. Nuovo Cimento B 53 (1979) 11–333.
[8] V. Benza, L.A. Lugiato, Dressed mode description of optical bistability, Z. Phys. B 35 (1979) 383–390.
[9] V. Benza, L.A. Lugiato, Dressed mode description of optical bistability: II. Analytical treatment of self-pulsing, Z. Phys. B 47 (1982) 79–93.
[10] L.A. Lugiato, L.M. Narducci, D.K. Bandy, C.A. Pennise, Self pulsing and chaos in a mean field model of optical bistability, Opt. Commun. 43 (1982) 281–286.
[11] L.A. Lugiato, L.M. Narducci, Single-mode and multimode instabilities in lasers and related optical systems, Phys. Rev. A 32 (1985) 1576–1587.
[12] S.S. Hassan, P.D. Drummond, D.F. Walls, Dispersive optical bistability in a ring cavity, Opt. Commun. 27 (1978) 480–484.
[13] P. Meystre, On the use of the mean field theory in optical bistability, Opt. Commun. 26 (1978) 227–280.
[14] E. Abraham, R.K. Bullough, S.S. Hassan, Space and time-dependent effects in optical bistability, Opt. Commun. 29 (1979) 109–114.
[15] E. Abraham, S.S. Hassan, R.K. Bullough, Dispersive optical bistability in a Fabry–Perot cavity, Opt. Commun. 33 (1980) 93–98;
E. Abraham, S.S. Hassan, Effects of inhomogeneous broadening on optical bistability in a Fabry–Perot cavity, Opt. Commun. 35 (1980) 291–297.
[16] C.M. Bowden, M. Ciftan, H.R. Robl (Eds.), Optical Bistability, Plenum press, New York, 1981.
[17] S.F. Hass, M. Sergent III, Effects of a squeezed vacuum on absorptive optical bistability, Opt. Commun. 79 (1990) 366–372.
[18] P. Galatola, L.A. Lugiato, M. Porreca, P. Tombesi, Optical switching by variation of the squeezing phase, Opt. Commun. 81 (1991) 175–178.
[19] S.M.A. Maize, M.F.M. Ali, S.S. Hassan, Squeezed vacuum effects on optical bistability in a Fabry–Perot cavity, Nonlinear Opt. 8 (1990) 219–230.
[20] J. Bergou, D. Zhao, Effects of a squeezed vacuum input on optical bistability, Phys. Rev. A 52 (1995) 1550–1560.
[21] S.S. Hassan, H.A. Batarfi, R. Saunders, R.K. Bullough, Bistable behaviour in squeezed vacua: I. Stationary analysis, Eur. Phys. J. D 8 (2000) 403–416.
[22] H.A. Batarfi, S.S. Hassan, R. Saunders, R.K. Bullough, Bistable behaviour in squeezed vacua: II. Stability analysis, Eur. Phys. J. D 8 (2000) 417–429.
[23] M.F.M. Ali, S.S. Hassan, S.M.A. Maize, Transverse field, squeezed vacuum and inhomogeneous broadening effects on optical bistability, J. Opt. B: Quantum Semiclass. Opt. 4 (2002) 388–395.
[24] S.S. Hassan, Y.A. Sharaby, Critical slowing down in a bistable model with squeezed vacuum environment, Eur. Phys. J. D 30 (2004) 393–401.
[25] L.P. Maia, G.A. Prataviera, S.S. Mizrahi, Optical bistability in sideband output modes induced by a squeezed vacuum, Phys. Rev. A 69 (2004) 053802–053808.
[26] H.A. Batarfi, Dispersive switching in bistable models, J. Nonlinear Opt. Phys. Mater. 17 (2008) 265–273.
[27] Y.A. Sharaby, S.S. Hassan, Dispersive switching in mesoscopic multistable systems, J. Nonlinear Opt. Phys. Mater. 17 (2008) 339–347.
[28] R.J. Ballagh, J. Cooper, M.W. Hamilton, W.J. Sandle, D.M. Warrington, Optical bistability in a Gaussian cavity mode, Opt. Commun. 37 (1981) 143–148.
[29] W.J. Sandle, R.J. Ballagh, A. Gallagher, Optical bistability experiments and mean field theories, in: C.M. Bowden, M. Ciftan, H.R. Robl (Eds.), Optical Bistability, Plenum, New York, 1981, pp. 93–108.
[30] E. Arimando, A. Gozzini, L. Lovitch, E. Pistelli, Microwave dispersive bistability in a confocal Fabry–Perot microwave cavity, in: C.M. Bowden, M. Ciftan, H.R. Robl (Eds.), Optical Bistability, Plenum, New York, 1981, pp. 151–171.
[31] P.D. Drummond, Optical bistability in a radially varying mode, IEEE J. Quantum Electron. 17 (1981) 301–306.
[32] P.D. Drummond, Applications of the generalized p-representation to optical bistability, in: C.M. Bowden, M. Ciftan, H.R. Robl (Eds.), Optical Bistability, Plenum, New York, 1981, pp. 481–501.
[33] L.A. Lugiato, M. Milani, Transverse effects and self-pulsing in optical bistability, Z. Phys. B 50 (1983) 171–179.
[34] F. Xijun, T. Baoguo, Y. Zhifang, W. Xiangtai, Inhomogeneously broadened ring-cavity optical bistability system with a Gaussian transverse intensity profile, Phys. Rev. A 44 (1991) 2048–2056.
[35] B.V. Thompson, J.A. Hermann, Modified optical bistability in two-photon absorption, Phys. Lett. A 83 (1981) 376–378.
[36] S.M.A. Maize, M.F.M. Ali, Stability of optical bistability for a standing wave cavity filled with a medium of mixed atomic species, Egypt, J. Phys. 26 (1995) 1–13.
[37] M.F.M. Ali, S.M.A. Maize, M.A. El-Deberky, Transverse field and inhomogeneous broadening effects on optical bistability in mixed species, Int. J. Mod. Phys. B 22 (2008) 3641–3653.

[38] Y.A. Sharaby, A. Joshi, S.S. Hassan, Optical bistability without the rotating wave approximation, Phys. Lett. A 374 (2010) 2188–2194.
[39] S.S. Hassan, Y.A. Sharaby, Mesoscopic multistability outside the rotating wave approximation, J. Phys. B: Atom. Mol. Opt. Phys. 41 (2008) 175502–175507.
[40] S.S. Hassan, Y.A. Sharaby, M.F.M. Ali, Bistabilities with higher harmonics in homogeneous and transverse effects, in press.
[41] D.F. Walls, Squeezed states of light, Nature 306 (1983) 41–146 ;; H. Vahlbruch et al., Observation of squeezed light with 10-dB quantum-noise reduction, Phys. Rev. Lett. 100 (2008) 033602–033611.